Electronic Supplementary Information

Enhanced stability of Cu^{2+}-ATCUN complex under physiologically relevant conditions by insertion of structurally bulky and hydrophobic amino acid residues into ATCUN motif

Takaaki Miyamoto,[a] Yuta Fukino,[a] Shinichiro Kamino,[ab] Masashi Ueda,[a] and Shuichi Enomoto*[ab]

[a] *Graduate School of Medicine, Dentistry, and Pharmaceutical Sciences, Okayama University, Okayama, Okayama 700-8530*
[b] *Next-generation Imaging Team, RIKEN-CLST, Kobe, Hyogo 650-0047*

Contents

1. Supplementary Tables and Figures

Table S1 Logarithms of overall protonation constants of ATCUN peptides.
Table S2 Logarithms of overall stability constants of Cu^{2+}-ATCUN complexes.
Table S3 Visible absorption spectroscopic data of $CuH_{-2}L$ species.
Table S4 CD spectroscopic data of $CuH_{-2}L$ species.
Table S5 Analytical data of ATCUN and ATCUN-Oct peptides.
Fig. S1 pH titration curves of Cu^{2+}-ATCUN complexes.
Fig. S2 Distribution diagrams of $CuH_{-2}L$ in aqueous solution.
Fig. S3 SEC-HPLC elution curves of ^{64}Cu-ATCUN complexes.
Fig. S4 SEC-HPLC elution curves of $^{nat}Cu^{2+}$-ATCUN complexes.
Fig. S5 SEC-HPLC elution curves of ^{64}Cu- and $^{nat}Cu^{2+}$-ATCUN-Oct complexes.
Fig. S6 SEC-HPLC elution curves of ^{64}Cu- and $^{nat}Cu^{2+}$-YYH-Oct complex.
Fig. S7 Visible absorption and CD spectra of Cu^{2+}-ATCUN-Oct complexes

2. Supplementary References

1. Supplementary Tables and Figures

Table S1 Logarithms of overall protonation constants of ATCUN peptides

Peptide	$\log \beta_{HL}$ [a] $L+H \rightleftarrows HL$ [b]	$\log \beta_{H2L}$ [a] $HL+H \rightleftarrows H_2L$ [b]	$\log \beta_{H3L}$ [a] $H_2L+H \rightleftarrows H_3L$ [b]	$\log \beta_{H4L}$ [a] $H_3L+H \rightleftarrows H_4L$ [b]
1 [c]	6.83 (0.006)	12.73 (0.005)	–	–
2 [c]	7.15 (0.004)	13.28 (0.004)	–	–
3 [c]	7.09 (0.003)	13.01 (0.003)	–	–
4 [c]	7.15 (0.015)	12.68 (0.019)	–	–
5 [c]	7.77 (0.007)	13.89 (0.008)	–	–
6 [c]	8.18 (0.010)	14.83 (0.010)	18.52 (0.014)	20.79 (0.032)
7 [d]	7.82 (0.003)	13.97 (0.004)	–	–
8 [d]	7.17 (0.004)	13.26 (0.004)	–	–
9 [d]	7.06 (0.003)	13.11 (0.003)	–	–

[a] Overall protonation constants ($\log \beta$) were determined by pH titration at 25 °C in 0.1 M KCl aqueous solution. Values in parentheses are standard deviations. [b] L represents a fully deprotonated peptide ligand. Charges are omitted for clarity. [c] Ref. S1. [d] This work.

Table S2 Logarithms of overall stability constants of Cu^{2+}-ATCUN complexes

Peptide	$\log \beta_{CuHL}$ [a] $Cu+H+L \rightleftarrows CuHL$ [b]	$\log \beta_{CuL}$ [a] $Cu+L \rightleftarrows CuL$ [b]	$\log \beta_{CuH-1L}$ [a] $Cu+L \rightleftarrows CuH_{-1}L+H$ [b]	$\log \beta_{CuH-2L}$ [a] $Cu+L \rightleftarrows CuH_{-2}L+2H$ [b]
1 [c]	–	–	3.53 (0.007)	−0.24 (0.002)
2 [c]	–	–	3.40 (0.020)	−0.20 (0.003)
3 [c]	–	–	3.16 (0.018)	−0.57 (0.004)
4 [c]	–	–	2.94 (0.013)	−1.11 (0.004)
5 [c]	–	–	2.78 (0.017)	−1.32 (0.003)
6 [c]	13.85 (0.005)	9.70 (0.010)	4.60 (0.004)	−0.93 (0.003)
7 [d]	–	–	3.33 (0.009)	−0.63 (0.002)
8 [d]	–	–	3.55 (0.009)	−0.38 (0.003)
9 [d]	–	–	3.20 (0.007)	− 0.62 (0.002)

[a] Overall stability constants were determined by pH titration at 25 °C in 0.1 M KCl aqueous solution. Values in parentheses are standard deviations. [b] L represents a fully deprotonated peptide ligand. Charges are omitted for clarity. [c] Ref. S1. [d] This work.

Table S3 Visible absorption spectroscopic data of $CuH_{-2}L$ species

	1[b]	**2**[b]	**3**[b]	**4**[b]	**5**[b]	**6**[b]	**7**[c]	**8**[c]	**9**[c]
pH	6.7	5.3	6.0	6.2	6.5	8.0	10.1	7.2	7.2
λ_{max} (nm)	526	518	523	523	522	526	530	516	533
ε (M^{-1} cm^{-1})[a]	113	106	110	108	110	109	95	99	105

[a] d-d transition. [b] Ref. S1. [c] This work.

Table S4 CD spectroscopic data of $CuH_{-2}L$ species

	1[d]	**2**[d]	**3**[d]	**4**[d]	**5**[d]	**6**[d]	**7**[e]	**8**[e]	**9**[e]
pH	6.0	5.7	5.5	5.8	6.9	9.6	10.6	7.7	8.1
λ (nm)	568	561	558	558	554	564	593	559	565
Δε (M^{-1} cm^{-1})[a]	−0.8	−0.8	−0.9	−0.9	−1.3	−0.8	−0.2	−0.8	−1.2
λ (nm)	489	483	480	477	475	484	504	484	483
Δε (M^{-1} cm^{-1})[a]	0.7	0.7	0.5	0.5	0.5	0.6	1.0	0.7	0.5
λ (nm)	311	312	306	307	312	308	303	317	311
Δε (M^{-1} cm^{-1})[b]	1.4	1.6	1.5	1.5	2.0	1.6	0.5	1.1	2.1
λ (nm)	271	269	269	269	272	271	273	268	271
Δε (M^{-1} cm^{-1})[c]	−3.0	−4.8	−3.2	−3.1	−4.8	−2.7	−0.2	−3.8	−4.7

[a] d-d transition. [b] $N^-_{(amide)} \rightarrow Cu^{2+}$ CT transition. [c] $NH_2 \rightarrow Cu^{2+}$ CT transition. [d] Ref. S1. [e] This work.

Table S5 Analytical data of ATCUN and ATCUN-Oct peptides

		$[M+H]^+$		$[M+2H]^{2+}$		$[M+3H]^{3+}$	
Peptide	Purity (%)[a]	Calcd	Found	Calcd	Found	Calcd	Found
1[e]	97	668	668[b]	334	–	223	–
2[e]	> 99	734	734[b]	367	–	245	–
3[e]	> 99	752	752[b]	376	–	251	–
4[e]	> 99	696	696[b]	348	–	232	–
5[e]	> 99	638	638[b]	319	–	213	–
6[e]	98	670	670[b]	335	–	224	–
7[f]	> 99	554	554[c]	277	277 [c]	185	–
8[f]	> 99	766	–	383	383[c]	256	–
9[f]	98	642	–	321	321[c]	214	–
NNH-Oct[f]	> 99	1385	–	692.8	692.8[d]	462.2	462.2[d]
VVH-Oct[f]	> 99	1355	–	677.8	677.8[d]	452.2	452.2[d]
DDH-Oct[f]	> 99	1387	–	693.8	693.8[d]	462.9	462.9[d]
GGH-Oct[f]	> 99	1271	–	635.8	–	424.2	424.2[d]
YYH-Oct[f]	> 99	1483	–	741.8	741.8[d]	494.9	494.9[d]
TTH-Oct[f]	> 99	1359	–	679.8	679.8[d]	453.5	453.5[d]

[a] Purity was determined by analytical HPLC. [b] Mass values were obtained from MALDI-TOF mass spectrometry. [c] Mass values were obtained from ESI mass spectrometry. [d] Mass values were obtained from high-resolution ESI mass spectrometry. [e] Ref. S1. [f] This work.

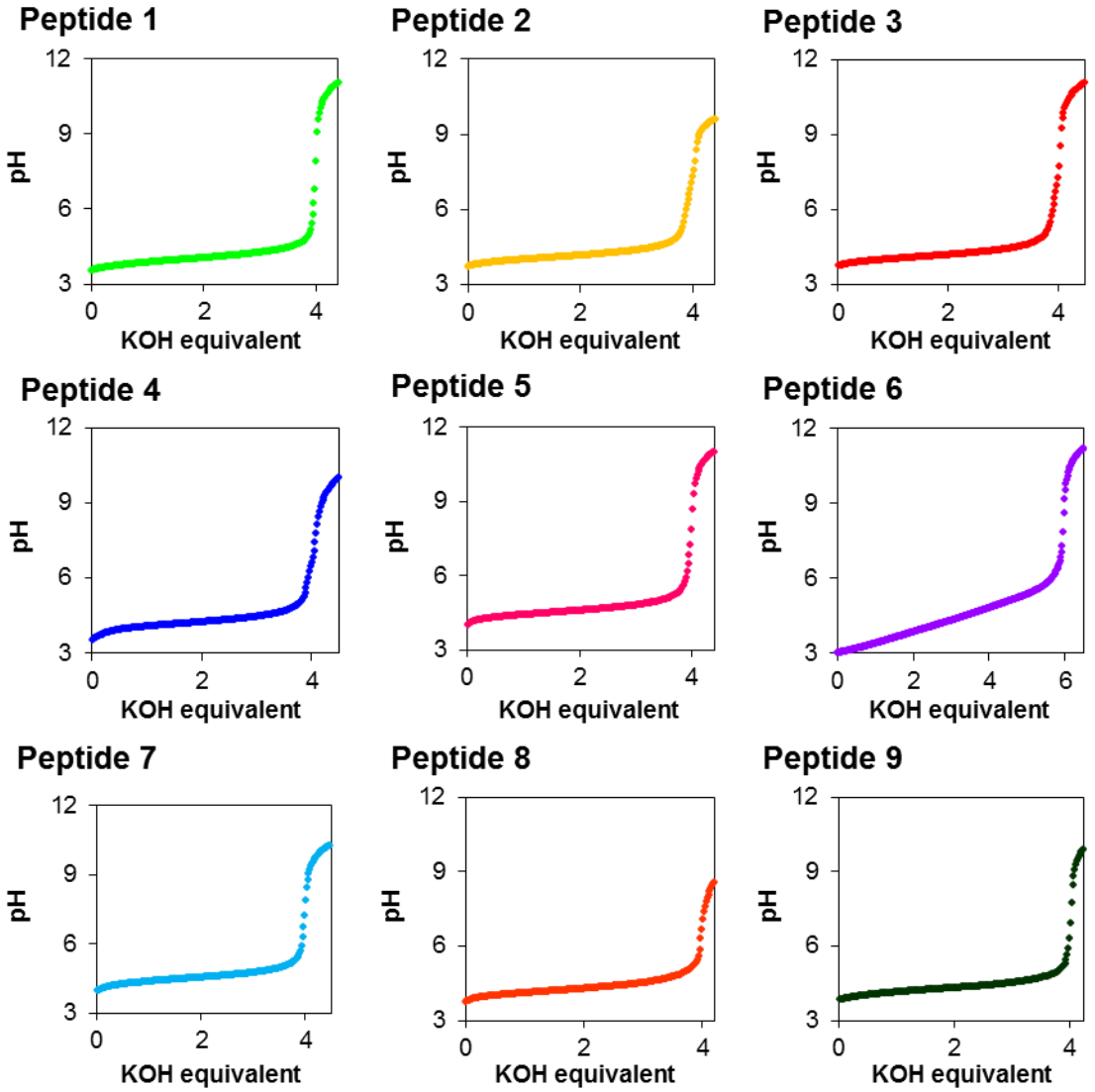

Fig. S1 pH titration curves of Cu^{2+}-ATCUN complexes. pH titration was performed at 25 °C over the pH range of 3–10 using a total sample volume of 10 mL, under argon or nitrogen atmosphere. Ionic strength was adjusted to 0.1 M with KCl. Peptide and Cu^{2+} concentration was 1.0 mM. Potassium hydroxide (KOH) solution (0.1 M) was used as titrant. KOH equivalent represents equivalent mole of KOH per Cu^{2+} ion.

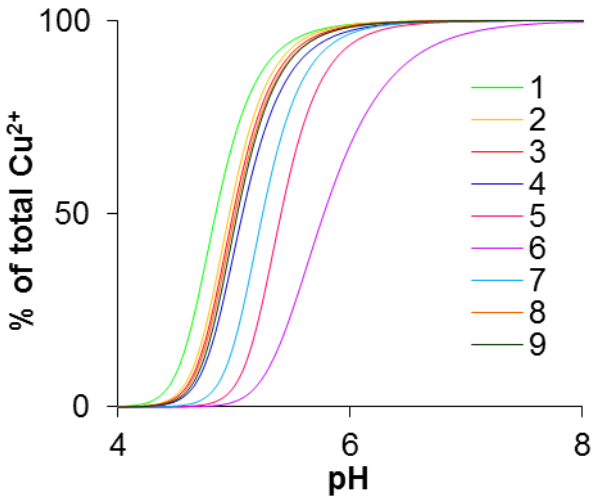

Fig. S2 Distribution diagrams of $CuH_{-2}L$ in aqueous solution. Conditions: temperature, 25 °C; KCl concentration, 0.1 M; peptide and Cu^{2+} concentration, 1.0 mM.

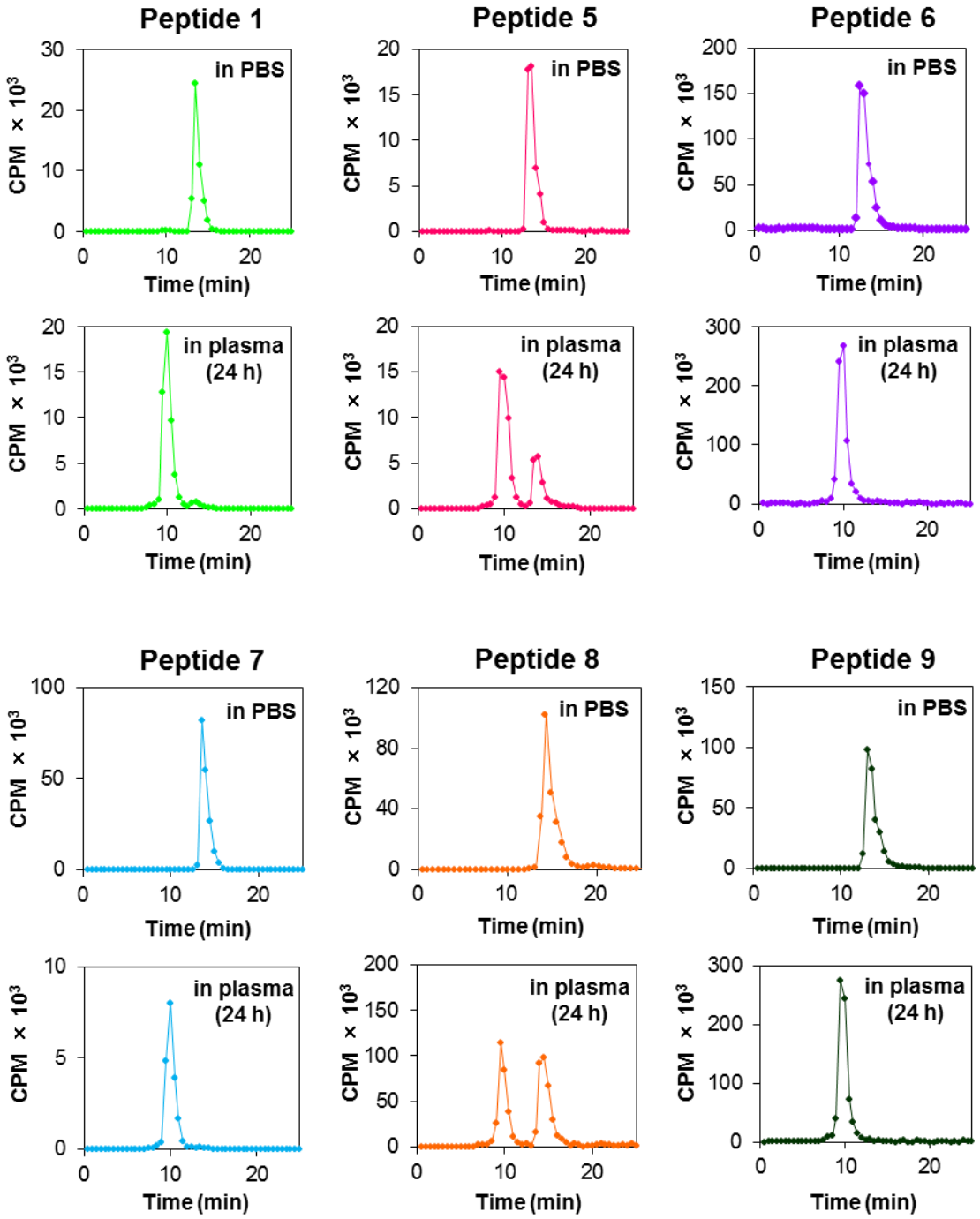

Fig. S3 SEC-HPLC elution curves of ^{64}Cu-ATCUN complexes. The complexes were analyzed before (in PBS) or after incubation at 37 °C for 24 h in plasma. Experimental conditions: instrument, LC-20AT pump and DGU-20A3 degasser (Shimadzu, Kyoto, Japan); column, TSKgel Super SW 2000 column (300 × 4.6 mm, 5 µm); solvent, 10 mM phosphate buffer containing 0.3 M NaCl; pH, 7.0; flow rate, 0.35 mL/min. Retention times of the complexes: ^{64}Cu-**1**, 13.5 min; ^{64}Cu-**5**, 13.0 min; ^{64}Cu-**6**, 12.5 min; ^{64}Cu-**7**, 13.5 min; ^{64}Cu-**8**, 14.0 min; ^{64}Cu-**9**, 13.0 min.

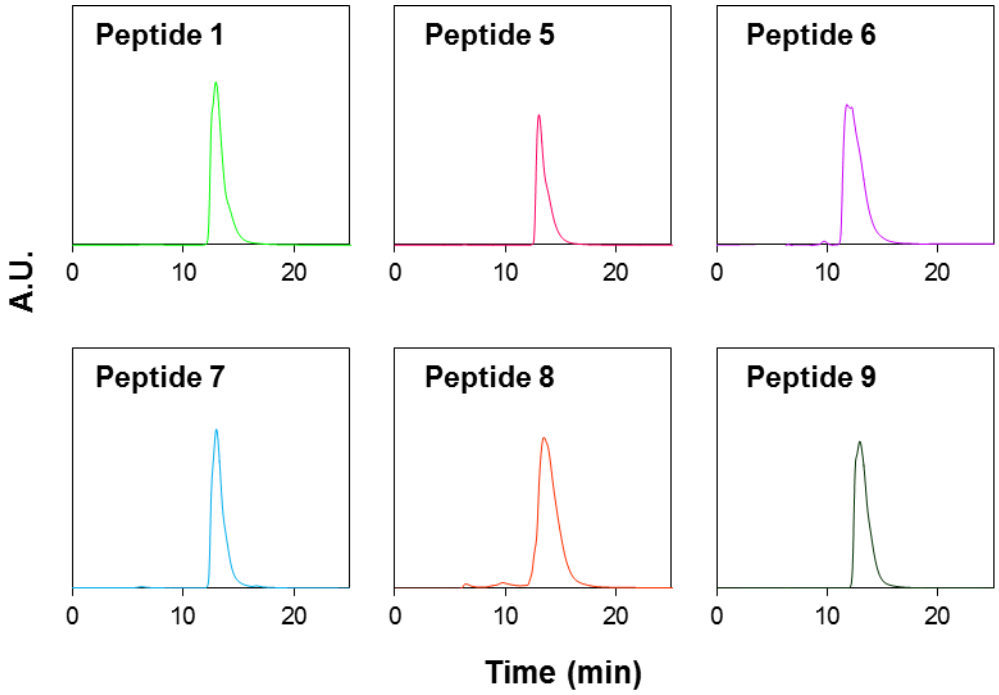

Fig. S4 SEC-HPLC elution curves of $^{nat}Cu^{2+}$-ATCUN complexes. Experimental conditions: instrument, PU-980 pump and UV-970 UV detector (Jasco, Tokyo, Japan); column, TSKgel Super SW 2000 column (300 × 4.6 mm, 5 µm); solvent, 10 mM phosphate buffer containing 0.3 M NaCl; pH, 7.0; flow rate, 0.35 mL/min; peptide-to-metal ratio, 1:1. Retention times of the complexes: Cu^{2+}-**1**, 12.9 min; Cu^{2+}-**5**, 13.0 min; Cu^{2+}-**6**, 12.0 min; Cu^{2+}-**7**, 13.0 min; Cu^{2+}-**8**, 13.5 min; Cu^{2+}-**9**, 12.9 min.

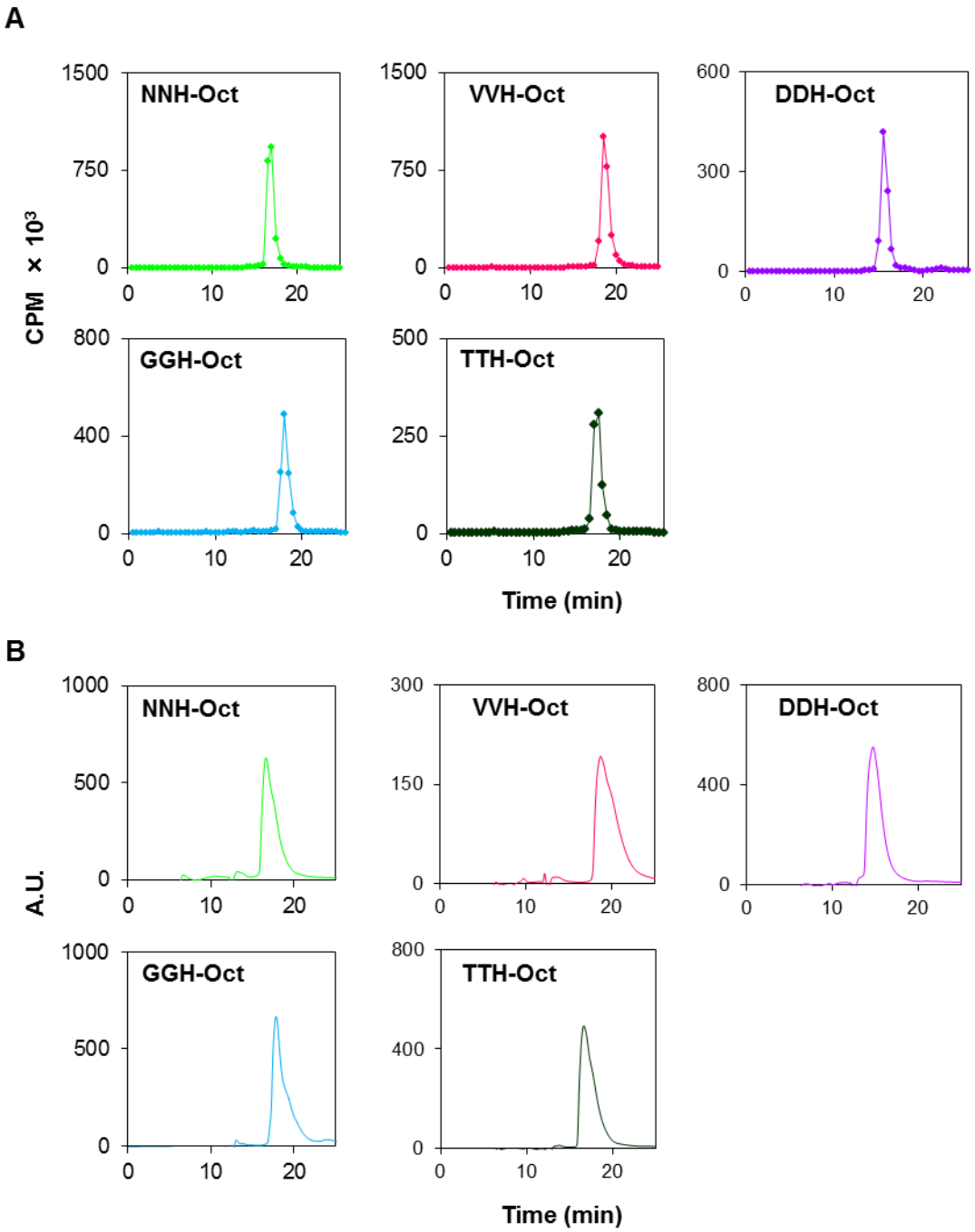

Fig. S5 SEC-HPLC elution curves of ^{64}Cu- (A) and $^{nat}Cu^{2+}$- (B) ATCUN-Oct complexes. Experimental conditions: instrument, LC-20AT pump and DGU-20A3 degasser (Shimadzu, Kyoto, Japan) (A), PU-980 pump and UV-970 UV detector (Jasco, Tokyo, Japan) (B); column, TSKgel Super SW 2000 column (300 × 4.6 mm, 5 μm); solvent, 10 mM phosphate buffer containing 0.3 M NaCl; pH, 7.0; flow rate, 0.35 mL/min; peptide-to-metal ratio, approximately 1000:1 (A) and 1:1 (B); detection, fractions (0.5 mL/tube) were collected and counted on a γ-counter (A), absorbance at 230 nm was monitored (B). Retention times of the complexes: NNH-Oct, 17.0 (A) and 16.6 (B) min; VVH-Oct, 18.5 (A) and 18.5 (B) min; DDH-Oct, 15.5 (A) and 14.6 (B) min; GGH-Oct, 18.0 (A) and 17.8 (B) min; TTH-Oct, 17.5 (A) and 16.7 (B) min. The small difference in retention times between ^{64}Cu- and $^{nat}Cu^{2+}$-complexes was responsible for the different experimental conditions.

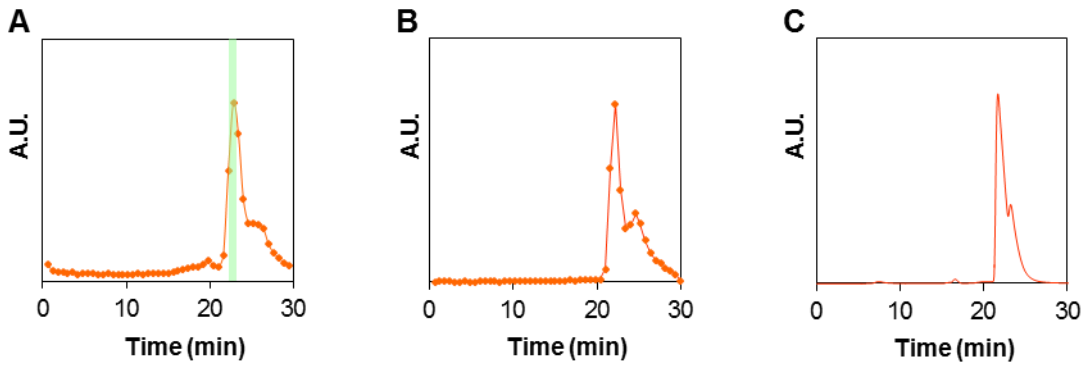

Fig. S6 SEC-HPLC elution curves of ^{64}Cu- and $^{nat}Cu^{2+}$-YYH-Oct complex. ^{64}Cu-YYH-Oct complex was purified by SEC-HPLC aftetr radiolabeling (A). Fractions eluting from 21.6 to 22.8 min in (A) (shown by the green column) were analyzed by SEC-HPLC (B). $^{nat}Cu^{2+}$-YYH-Oct complex was also analyzed by SEC-HPLC (C). Experimental conditions: instrument, LC-20AT pump and DGU-20A3 degasser (Shimadzu, Kyoto, Japan) (A and B), PU-980 pump and UV-970 UV detector (Jasco, Tokyo, Japan) (C); column, TSKgel Super SW 2000 column (300 × 4.6 mm, 5 µm); solvent, 10 mM phosphate buffer containing 0.3 M NaCl; pH, 7.0; flow rate, 0.35 mL/min; injected sample, a mixture of $^{64}CuCl_2$ and YYH-Oct (approximately 1:1000) (A), fractions eluted from 21.6 to 22.8 min (B), a mixture of $Cu(NO_3)_2$ and peptide (1:1) (C); detection, fractions (0.6 mL/tube) were collected and counted on a γ-counter (A and B), and absorbance at 230 nm was monitored (C).

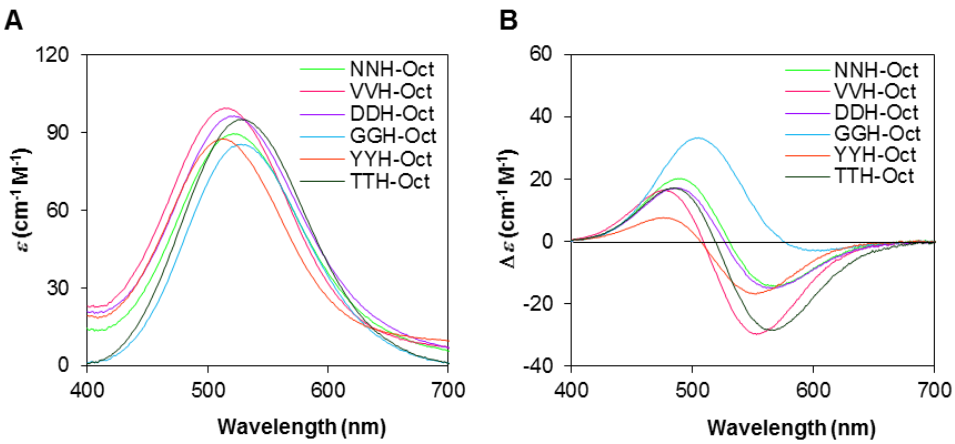

Fig. S7 Visible absorption (A) and CD (B) spectra of Cu^{2+}-ATCUN-Oct complexes. Mesurement conditions: peptide and Cu^{2+} concentration, 1.0 mM; solvent, PBS; pH, 7.4.

2. Supplementary References

S1) T. Miyamoto, S. Kamino, A. Odani, M. Hiromura and S. Enomoto, *Chem*. *Lett*., 2013, **42**, 1099–1101.